JGR Atmospheres

RESEARCH ARTICLE
10.1029/2020JD033418

Understanding Tropical Convection Through Triple Oxygen Isotopes of Precipitation From the Maritime Continent

Shaoneng He[1], Dominik Jackisch[1], Dhrubajyoti Samanta[2], Phyllis Kho Yu Yi[2], Guangxin Liu[3], Xianfeng Wang[1,2], and Nathalie F. Goodkin[1,2,4]

[1]Earth Observatory of Singapore, Nanyang Technological University, Singapore, [2]Asian School of the Environment, Nanyang Technological University, Singapore, [3]Yunnan Key Laboratory of Earth System Science, Yunnan University, Kunming, China, [4]Division of Physical Sciences, American Museum of Natural History, New York, NY, USA

Key Points:

- Monthly tropical precipitation in Singapore exhibits a weak amount effect
- Regional convection has different impacts on precipitation $\delta^{18}O$, d-excess, and ^{17}O-excess
- Processes during transport and precipitation have modified ^{17}O-excess, which no longer records the relative humidity in moisture source regions

Supporting Information:

- Supporting Information S1

Correspondence to:

S. He,
snhe@ntu.edu.sg; heshaoneng@gmail.com

Citation:

He, S., Jackisch, D., Samanta, D., Yi, P. K. Y., Liu, G., Wang, X., & Goodkin, N. F. (2021). Understanding tropical convection through triple oxygen isotopes of precipitation from the maritime continent. *Journal of Geophysical Research: Atmospheres*, *126*, e2020JD033418. https://doi.org/10.1029/2020JD033418

Received 5 JUL 2020
Accepted 4 DEC 2020

Author Contributions:

Conceptualization: Shaoneng He, Nathalie F. Goodkin
Data curation: Shaoneng He, Dominik Jackisch, Dhrubajyoti Samanta, Phyllis Kho Yu Yi, Guangxin Liu, Xianfeng Wang
Formal analysis: Shaoneng He, Dominik Jackisch, Phyllis Kho Yu Yi
Funding acquisition: Shaoneng He, Nathalie F. Goodkin
Investigation: Shaoneng He, Dominik Jackisch

Abstract Monthly precipitation samples from Singapore were collected between 2013 and 2019 for stable isotope analysis to further our understanding of the drivers of tropical precipitation isotopes, in particular, ^{17}O-excess. $\delta^{18}O$ ranges from −11.34‰ to −2.34‰, with a low correlation to rainfall ($r = -0.31$, $p = 0.014$), suggesting a weak amount effect. d-excess is relatively consistent and has an average value of 10.89‰ ± 3.45‰. Compared to high-latitude regions, ^{17}O-excess in our samples generally falls in a narrower range from 2 to 47 per meg with an average of 21 ± 11 per meg. Moreover, ^{17}O-excess shows strong periodic variability; spectral analysis reveals 3-month, 6-month, and 2.7-year periodicities, likely corresponding to intraseasonal oscillations, monsoons, and the El Niño–Southern Oscillation (ENSO), respectively. In contrast, d-excess shows no clear periodicities. Although spectral analysis only identifies 6-month periodicity in the $\delta^{18}O$ time series, $\delta^{18}O$ tracks the Nino3.4 sea surface temperature variability; the average $\delta^{18}O$ value (−5.2‰) is higher during El Niño years than ENSO neutral years (−7.6‰). Therefore, regional convection associated with monsoons and ENSO has different impacts on $\delta^{18}O$, d-excess, and ^{17}O-excess. ^{17}O-excess and d-excess are anticorrelated and do not relate to the relative humidity in moisture source regions. Extremely low humidity and drought conditions in moisture source regions would be required to account for high ^{17}O-excess. Processes during transport and precipitation likely modify these two parameters, especially ^{17}O-excess, which no longer record humidity conditions of moisture source regions. Our findings will be useful for further modeling studies to identify physical processes during convection that alter d-excess and ^{17}O-excess.

1. Introduction

Water stable isotopes ($\delta^{18}O$ and $\delta^{2}H$) are considered as natural tracers of hydrological cycles because water isotopes fractionate (through equilibrium and kinetic fractionations) during phases change and diffusive processes. Precipitation $\delta^{18}O$ and $\delta^{2}H$ have been related to local environmental or climatic conditions at sampling sites, for example, a positive correlation between precipitation isotope values and temperature at midlatitudes to high latitudes (temperature effect), and an anticorrelation between precipitation amount and isotope values in subtropical and tropical regions (amount effect). These isotope–climate relationships have been applied to interpret paleoclimate records, such as ice cores and speleothems, and help us to understand past climate change (e.g., Cheng et al., 2016; Hoffmann et al., 2003; Jouzel, 2003; Klein et al., 2016). In more recent investigations of tropical precipitation, particularly on daily and event time scales, extremely weak or no correlation is found between stable isotopes and rainfall (e.g., He, Goodkin, Jackisch, et al., 2018; He, Goodkin, Kurita, et al., 2018; Kurita et al., 2009; Lekshmy et al., 2014; Moerman et al., 2013; Vimeux et al., 2011). The stable isotopes in the event or daily precipitation are largely controlled by the convective activities, precisely the integration of convective activities or accumulative convective activities prior to the precipitation (He, Goodkin, Jackisch, et al., 2018; Vimeux et al., 2011). Thus, the amount effect appears in a regional scale not in daily or event scales. Observations and model simulations indicate that cloud microphysics and cloud types have significant influence on precipitation stable isotopes (Munksgaard et al., 2019; Risi et al., 2008; Tremoy et al., 2014). Isotope-enabled general circulation models (GCMs) have also been used in stable isotope studies of precipitation. However, while these GCMs reproduce the global distribution of mean annual isotopes in precipitation reasonably well, they tend to overestimate the

Methodology: Shaoneng He
Project Administration: Shaoneng He
Resources: Shaoneng He, Dhrubajyoti Samanta
Supervision: Shaoneng He, Nathalie F. Goodkin
Validation: Shaoneng He
Writing – original draft: Shaoneng He
Writing – review & editing: Shaoneng He, Dominik Jackisch, Dhrubajyoti Samanta, Phyllis Kho Yu Yi, Guangxin Liu, Xianfeng Wang, Nathalie F. Goodkin

correlation between isotopes and rainfall amount in tropical regions (Kurita et al., 2009; Lee et al., 2007; Risi, Bony, et al., 2010). These discrepancies reflect the complexities of atmospheric and climatic processes in tropical regions and our limited understanding of the controls of stable isotopes in tropical precipitation.

Deuterium excess, defined as d-excess = $\delta^2H - 8*\delta^{18}O$, is commonly considered a tracer of evaporation conditions of moisture source regions, in particular, relative humidity (RH) (Benetti et al., 2014; Merlivat & Jouzel, 1979). Jouzel et al. (1982) used d-excess in polar ice to explain past humidity changes in ocean source regions. Later, source region surface temperature was considered a dominant control (Stenni, 2001; Vimeux et al., 2001), and d-excess was used to trace the change in moisture sources (e.g., He, Goodkin, Jackisch, et al., 2018; Voss et al., 2018). Aemisegger et al. (2014) even used d-excess as a proxy for continental moisture recycling and plant transpiration. However, d-excess is very sensitive to both equilibrium and kinetic fractionations during moisture transport and precipitation, and thus is not a conservative tracer (Schoenemann et al., 2014, and the references therein), making it impossible to infer climatic conditions at ocean source regions using d-excess alone.

A promising new tracer of the hydrological cycle is ^{17}O-excess, which can be reliably calculated ($^{17}O\text{-excess} = \ln(\delta^{17}O + 1) - 0.528 \times \ln(\delta^{18}O + 1)$) by precisely measuring the third oxygen isotope ^{17}O owing to recent advances in analytical techniques (Barkan & Luz, 2005) and instruments (Steig et al., 2014). Laboratory experiments and theory show that ^{17}O-excess in precipitation is primarily controlled by source vapor evaporation and is negatively correlated with RH (Angert et al., 2004; Barkan & Luz, 2007; Landais et al., 2008, 2010; Risi et al., 2013). In contrast to d-excess, ^{17}O-excess is independent of temperature and therefore could be a more reliable tracer of RH in moisture source regions.

Current studies of ^{17}O-excess mostly focused on snow and ice cores in high-latitude regions (e.g., Landais et al., 2008; Landais, Ekaykin, et al., 2012; Landais, Steen-Larsen, et al., 2012; Miller, 2018; Pang et al., 2015; Schoenemann & Steig, 2016; Schoenemann et al., 2014; Winkler et al., 2012). Consistent ^{17}O-excess of surface snow along a transect between Terra Nova Bay and Dome C in Antarctica, despite large changes in temperature with elevation, led Landais et al. (2008) to conclude that snow conserved the ^{17}O-excess signature of moisture and thus to interpret a 20 per meg increase in Vostok ice core ^{17}O-excess as a significant decrease (about 20%) in oceanic source region RH during the last deglaciation. However, such a large change in RH over the ocean is not realistic and contradicts modeling studies, and in addition, a part of the change can be attributed to the seasonal effect (Landais, Steen-Larsen, et al., 2012). Further, a large increase in ^{17}O-excess during the last deglaciation has only been observed at Vostok and thus is a local phenomenon (Jouzel et al., 2013; Winkler et al., 2012). More recent studies have shown that kinetic fractionation associated with supersaturation under low-temperature conditions is the primary control of ^{17}O-excess in Antarctic precipitation (e.g., Landais, Steen-Larsen, et al., 2012; Risi et al., 2013; Schoenemann et al., 2014). Pang et al. (2015) suggests that supersaturation effects on ^{17}O-excess vary spatially in Antarctica and cannot be simply explained by supersaturation nor solely by moisture source RH change.

Compared to high-latitude regions, studies on ^{17}O-excess of precipitation in subtropical and tropical regions are sparse. Tian et al. (2018) showed that ^{17}O-excess of rainfall and snowfall in the central United States recorded evaporation conditions at the moisture source. Uechi and Uemura (2019) examined triple oxygen isotopes of precipitation on a subtropical island and found that ^{17}O-excess of precipitation also reflects the variation in the RH at the moisture source region. An investigation of African monsoon precipitation by Landais et al. (2010) is the only study on ^{17}O-excess of tropical precipitation and the results implied that rain evaporation significantly affects ^{17}O-excess of tropical precipitation. A GCM simulation (Risi et al., 2013) highlights that rain reevaporation and convection are the major processes impacting ^{17}O-excess in the tropics. In general, our knowledge about what controls ^{17}O-excess in tropical precipitation is very poor. Before applying ^{17}O-excess as a tracer of hydrological processes in tropical regions, more studies, especially observations, are needed to help us identify the factors or processes that control ^{17}O-excess in precipitation and its spatial–temporal variations.

In this study, we collected monthly precipitation in Singapore between 2013 and 2019. We analyzed these samples for their stable isotope compositions and compared $\delta^{18}O$ and two secondary parameters, d-excess and ^{17}O-excess, with on-site meteorological parameters and normalized RH of ocean moisture source regions. Our objectives are (1) to investigate what controls the temporal variation of $\delta^{18}O$ and, in particular,

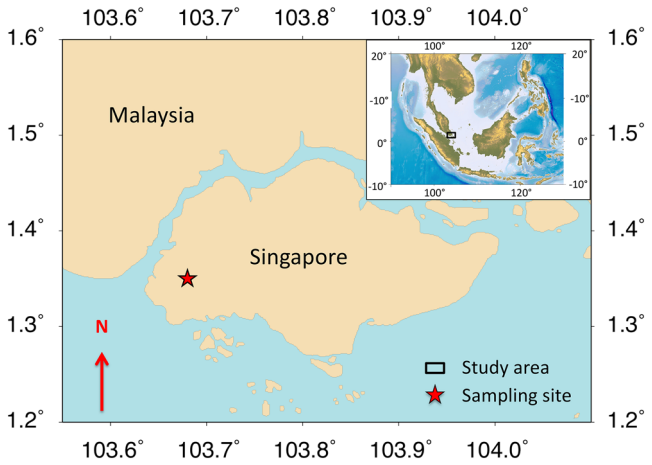

Figure 1. Map of Singapore with the sampling site (★) at Nanyang Technological University (1.35°N, 103.68°E, altitude of 40 m above sea level).

^{17}O-excess in monthly precipitation and (2) to explore whether ^{17}O-excess can be used as a tracer of ocean source region RH in tropical regions. Our study provides a unique data set from tropical regions to validate isotope-enabled GCMs, particularly those incorporating δ^{17}O and ^{17}O-excess, and contributes to advancing our knowledge of the key processes that drive precipitation isotopes in the tropics.

2. Materials and Methods

2.1. Rain Station

Our rain station was installed on the top of the building that hosts Earth Observatory of Singapore (EOS) and the Asian School of the Environment, Nanyang Technological University (NTU) (Figure 1). We used the PALMEX rain collector, which was designed and tested by the IAEA in collaboration with the University of Rijeka (Gröning et al., 2012). Monthly rainwater samples were stored in 60 ml high-density polyethylene bottles and kept at 4°C prior to analysis.

2.2. Regional Climate

Singapore is an island city-state in Southeast (SE) Asia, located just north of the equator and at the southern tip of the Malay Peninsula (Figure 1). It has a tropical climate with abundant rainfall and uniform high temperature and humidity all year round. The climate of Singapore and neighboring countries is strongly shaped by two alternating monsoons, the Southwest (SW) monsoon (between June and September) and the Northeast (NE) monsoon (between December and March). During the SW monsoon, the dominant wind directions are southwesterly and southeasterly (Figure 2(a)), with the major moisture sources from the Indian Ocean and the Java Sea. During the NE monsoon, the northerly to northeasterly winds are prevalent (Figure 2(c)) and moisture mainly originates in the South China Sea (SCS). During two intermonsoon periods (April–May and October–November), there is no dominant wind and thus moisture comes from all directions (Figures 2(b) and 2(d)).

A distinct feature of the NE monsoon is a cold surge driven by the Siberian high. The NE cold surge can bring several days of continuous and widespread rain to the region. On the other hand, the SW monsoon in Singapore is characterized by the frequent occurrence of early-morning organized bands of thunderstorms that extend for hundreds of kilometers, also known as Sumatra Squalls (He, Goodkin, Kurita, et al., 2018; Lo & Orton, 2016). There are no distinct dry and wet seasons in Singapore though higher rainfall occur during the two monsoons.

2.3. Stable Isotope Measurement

A Picarro L2140-*i* water analyzer, a cavity ring-down spectrometer, was used to measure the stable isotope values (δ^{18}O, δ^{17}O, and δ^{2}H) of precipitation samples. We followed the procedure developed by van Geldern and Barth (2012) for instrument setup, referencing techniques, and memory and drift correction. A longer analytical time than that typically for the analysis of δ^{18}O and δ^{2}H only is required to obtain precise δ^{17}O and thus ^{17}O-excess values (Uechi & Uemura, 2019). This can be achieved by multiple injections with a longer integration time per injection. In our laboratory, each sample was analyzed 3 times with 16 injections each time (i.e., more than 2 h of analytical time for each time and 48 injections in total for each sample). ^{17}O-excess is defined by the following equation (Barkan & Luz, 2007):

$$^{17}\text{O-excess} = \ln(\delta^{17}\text{O} + 1) - 0.528 \times \ln(\delta^{18}\text{O} + 1)$$

where ^{17}O-excess is expressed in per meg (10^{-6}).

Early studies reported δ^{17}O and ^{17}O-excess without normalization to SLAP due to the lack of a consensus δ^{17}O value for SLAP, leading to discrepancies in measurement between laboratories (Barkan & Luz, 2007;

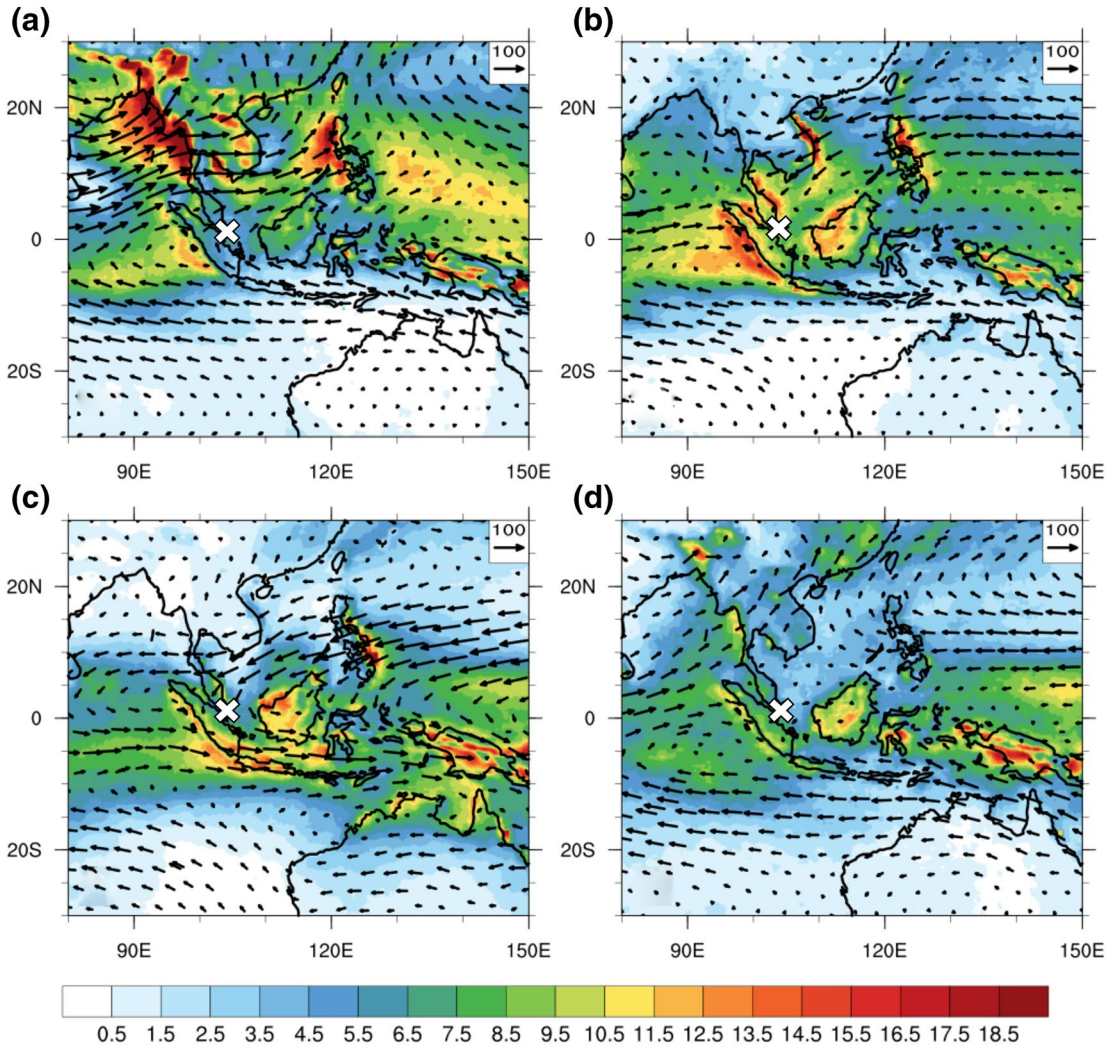

Figure 2. Regional moisture flux at 850 hPa (vector, in (g/kg)*(m/s)) and climatological precipitation (shaded, in mm/day) over 21 years between 1998 and 2018: (a) June–September, (b) October–November, (c) December–February, and (d) April–May. "×" represents the sampling site.

Landais et al., 2008; Luz & Barkan, 2010; Schoenemann et al., 2013). We use the value (−26.6968‰) proposed by Schoenemann et al. (2013) for SLAP $\delta^{17}O$ and normalize our data to the VSMOW-SLAP scale. In-house standards (KONA and TIBET), which are well calibrated against international references VSMOW2 and SLAP2, were used to calibrate the raw data in our laboratory. They have $\delta^{18}O$, $\delta^{17}O$, and $\delta^{2}H$ values ranging from 0‰ to −20‰, 0‰ to −10‰, and 0‰ to −144‰, respectively (Table S1). Long-term analysis of our quality assurance/quality control standard (OrgAu) yields a precision of 0.04‰ for $\delta^{18}O$, 0.2‰ for $\delta^{2}H$, 0.02‰ for $\delta^{17}O$, and 6 per meg for ^{17}O-excess.

2.4. Meteorological Data

We used a HOBO Data Logging Rain Gauge to record the on-site temperature (T), RH, and rainfall amount. The gauge, installed beside the rain station, is a battery-powered data collection system.

Monthly rainfall data between 1998 and 2019 were taken from merged satellite observations (TRMM/TMPA 3B43), with a horizontal resolution of 0.25° × 0.25° (https://giovanni.gsfc.nasa.gov/giovanni/#service=TmAvMp&starttime=&endtime=&dataKeyword=TRMM_3B43). Monthly winds components, specific humidity (for moisture flux calculation), and RH were taken from ECMWF ERA5 data sets, the most updat-

ed reanalysis products with a spatial resolution of 0.25° × 0.25° (www.ecmwf.int/en/forecasts/datasets/reanalysis-datasets/era5).

Monthly Climate Prediction Center (CPC) Oceanic Niño Index (ONI) was obtained from National Oceanic and Atmospheric Administration (NOAA) CPC National Weather Service (www.cpc.ncep.noaa.gov/data/indices/sstoi.indices). ONI is based on sea surface temperature (SST) anomalies from the climatological SST in the Niño 3.4 regions. Outgoing longwave radiation (OLR) is used from the NOAA products (https://www.ncdc.noaa.gov/cdr/atmospheric) with a horizontal resolution of 1° × 1°.

2.5. Spectral Analysis of Stable Isotopic Signals

We applied spectral analysis to the stable isotope data to identify the frequency of significant periodic variation in stable isotope signals of monthly rainwater over the study period. To further isolate and observe variability specific to significant frequencies (above 90% and 95%), a Gaussian filter using the Analyseries software (Paillard et al., 1996) was applied.

2.6. Back Trajectory Analysis

Back trajectory analysis was used to delineate the moisture source regions. The air mass back trajectories were calculated using the Hybrid Single-particle Lagrangian Integrated Trajectory (HYSPLIT) model (Stein et al., 2015). All the trajectories were initiated daily at 6 h intervals at 850 hPa level and traced back for 96 h. We also applied cluster analysis to the trajectories arriving at our sampling site to examine the seasonal variability of air masses (He, Goodkin, Jackisch, et al., 2018).

3. Results

3.1. $\delta^{18}O$ and Rainfall Amount

Monthly precipitation samples were collected between November 2013 and April 2019, and their isotope values, including d-excess and ^{17}O-excess, with the corresponding on-site meteorological parameters are listed in Table S2. In general, $\delta^{18}O$ shows large variation, ranging from –11.34‰ to –2.34‰. $\delta^{18}O$, along with rainfall, also exhibits a strong seasonal variability in the time series (Figure 3). Each year, precipitation has a lower $\delta^{18}O$ value during the periods around the two monsoons (Figure S1(a)). Correspondingly, higher rainfall was observed during these periods (Figure S1(b)). The spectral analysis of $\delta^{18}O$ also reveals significant periodicities at the 6-month bands (Figure 4).

NE monsoon rainfall increased over the last few years (Figure S1), suggesting an increase in convective activities. In the time series, variation in $\delta^{18}O$ follows the general pattern of ONI (Figure 3(a)). $\delta^{18}O$ tends to shift to higher values with an increase in ONI and to more negative values with a decrease in ONI.

In tropical and subtropical regions, $\delta^{18}O$ of monthly or yearly precipitation was found to be significantly related to rainfall amount, that is, the amount effect (e.g., Dansgaard, 1964; Rozanski et al., 1993). Surprisingly, only a weak negative correlation ($r = -0.31$ and $p = 0.01$) is observed between rainfall and $\delta^{18}O$ in this study (Figure S1).

3.2. d-Excess and ^{17}O-Excess

d-Excess is relatively consistent averaging around 10‰ with only a few values below 5‰. Seasonal variability in d-excess is not as strong as $\delta^{18}O$, and spectral analysis of d-excess only identifies weak 6-month periodicity with 90% confidence (Figure 4(b)). Event precipitation samples at our site were found to show seasonal variability in d-excess, reflecting the alternating moisture sources from the SCS to the Indian Ocean and the Java Sea (see Figure 5 in He, Goodkin, Jackisch, et al., 2018). Likely, monthly precipitation has blurred the seasonal variability signal in d-excess to some extent because it averages daily precipitation over a month and thus the amplitude of variability in daily precipitation isotopes is significantly reduced. In general, samples from January to March have lower d-excess values compared to the other months in each

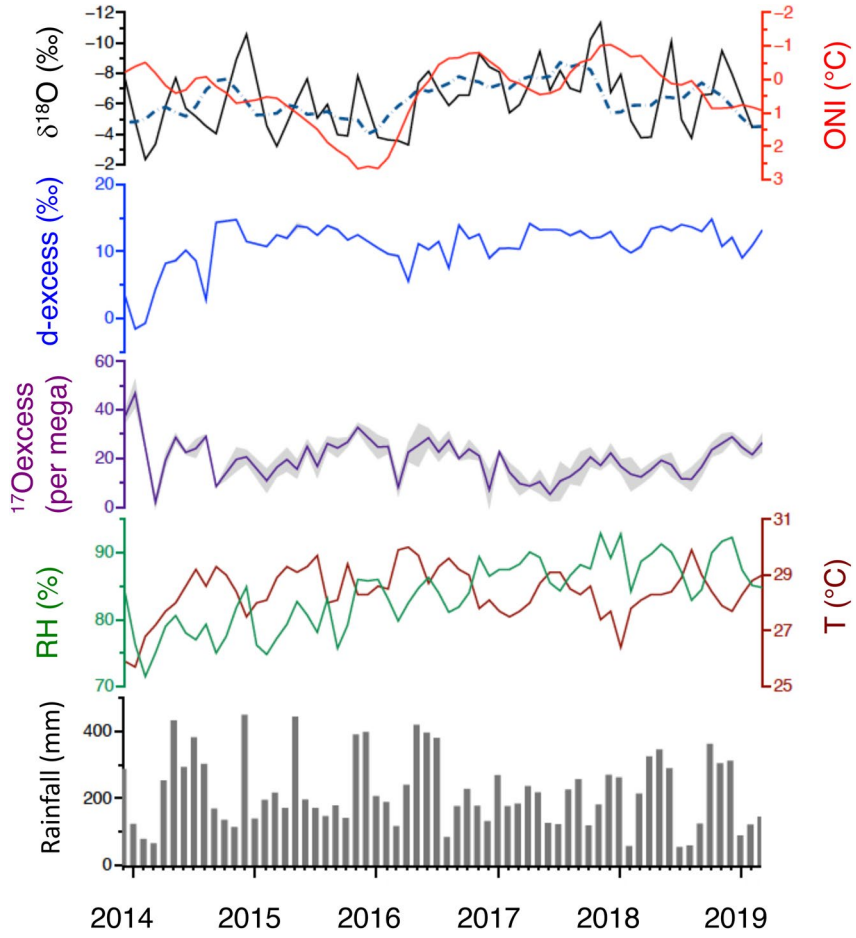

Figure 3. Times series of monthly precipitation $\delta^{18}O$ (black), d-excess (blue), ^{17}O-excess (purple), and rainfall (black bar) with on-site T (brown) and RH (green). ONI is also presented. Sample collected in November 2018 is not included in ^{17}O-excess curve because its ^{17}O-excess value of 80 per meg is much larger than the other samples. Dashed line represents 6-month running mean of $\delta^{18}O$. RH, relative humidity; ONI, Oceanic Niño Index.

year (Table S2). February is the driest month with the lowest rainfall amount in Singapore (Figure S1), and January and March are also relatively drier compared to other months. During this period, the subcloud rain evaporation is likely higher, leading to higher $\delta^{18}O$ but lower d-excess observed in the precipitation.

Compared to precipitation in high-latitude regions, our samples have a narrower range of ^{17}O-excess from 2 to 47 per meg, with the majority (>80%) between 10 and 30 per meg (Figure 5 and Table S2) except one sample collected in November 2018, which has an extremely high value of 80 per meg. Our samples have an average of 21 ± 11 per meg, similar to the precipitation from subtropical regions, whose ^{17}O-excess ranges from −5 to 54 per meg, with an average of 22 ± 11 per meg (Li et al., 2015; Tian et al., 2018; Uechi & Uemura, 2019). In higher latitudes, especially polar region, ^{17}O-excess of precipitation exhibits much larger variation, ranging from −35 to 70 per meg (Figure 5) due to kinetic fractionation at very low temperatures (Landais, Ekaykin, et al., 2012; Landais, Steen-Larsen, et al., 2012). Unlike d-excess, ^{17}O-excess in our samples shows strong periodic variability; the spectral analysis reveals significant 3-month, 6-month, and 2.7-year periodicities (Figure 4).

3.3. Correlation of $\delta^{18}O$, d-Excess, and ^{17}O-Excess with On-Site T and RH

$\delta^{18}O$ correlates to on-site RH but not to T, and d-excess weakly correlates to both T and RH (Figure S2). In contrast, ^{17}O-excess does not correlate to on-site T and RH at all, nor to RH at different levels of the atmosphere above Singapore region (Figure S3). Various correlations exist among $\delta^{18}O$, d-excess, and ^{17}O-excess. For example, no correlation is observed between $\delta^{18}O$ and ^{17}O-excess ($r = 0.16$ and $p = 0.222$), while a signif-

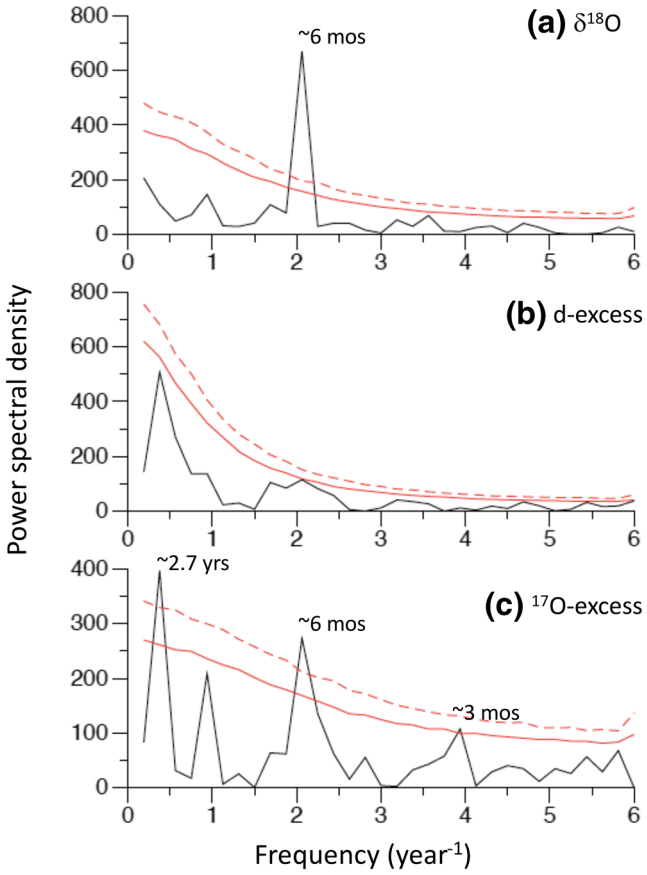

Figure 4. Spectral analysis of time series of $\delta^{18}O$ (a), d-excess (b), and ^{17}O-excess (c). Red solid line = 90% confidence, and red dashed line = 95% confidence.

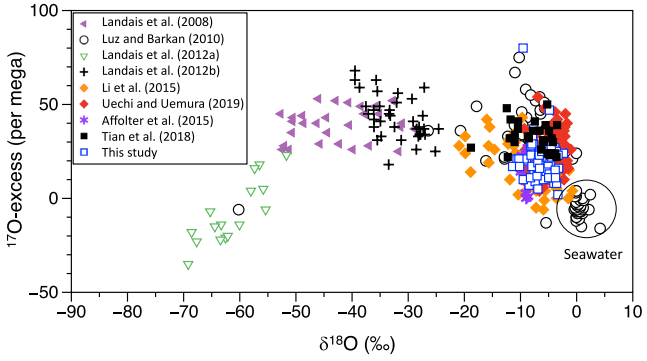

Figure 5. ^{17}O-excess versus $\delta^{18}O$ of monthly precipitation in this study in comparison with meteoric water samples reported in previous studies. ^{17}O-excess of seawater (in big circle) from Luz and Barkan (2010) was also shown.

icant negative correlation exists between $\delta^{18}O$ and d-excess (r = -0.35 and p = 0.006). There is an anticorrelation between d-excess and ^{17}O-excess (r = –0.36 and p = 0.005; Figures S2 and S4), which increases to r = –0.80 after excluding data of the months related to El Niño events, including 2015, the first 6 months in 2016 and December 2018 to April 2019.

4. Discussion

4.1. Local Meteoric Water Line

4.1.1. Local Meteoric Water Line for $\delta^{18}O$ and $\delta^{2}H$

The least squares regression analysis of monthly precipitation $\delta^{18}O$ and $\delta^{2}H$ defines a local meteoric water line (LMWL) for the study area (Figure 6(a)):

$$\delta^{2}H = 7.4957\ (\pm 0.2021)\delta^{18}O + 7.7295\ (\pm 1.3366)\ (R^{2} = 0.9587)$$

Monthly weighted average $\delta^{18}O$ and $\delta^{2}H$ values produce a similar LMWL (see Supporting Information for the calculation of monthly weighted average δ values):

$$\delta^{2}H = 7.6933\ (\pm 0.4406)\delta^{18}O + 6.8818\ (\pm 2.3031)\ (R^{2} = 0.9723)$$

The LMWL defined by monthly $\delta^{18}O$ and $\delta^{2}H$ is similar to the LMWL defined by daily precipitation $\delta^{18}O$ and $\delta^{2}H$ (He, Goodkin, Kurita, et al., 2018). Both the slope and intercept of Singapore LMWL are shallower than that of the global meteoric water line (GMWL) (Craig, 1961; Rozanski et al., 1993). This feature reflects the subcloud evaporation of raindrops, a very important process during tropical convection. Simulation and observation indicate that the reevaporation of falling rain under the clouds is one of several processes that affect tropical precipitation δ values (e.g., He, Goodkin, Jackisch, et al., 2018; He, Goodkin, Kurita, et al., 2018; Risi et al., 2008).

4.1.2. Local Meteoric Water Line for $\ln(\delta^{17}O + 1)$ and $\ln(\delta^{18}O + 1)$

$\ln(\delta^{17}O + 1)$ and $\ln(\delta^{18}O + 1)$ of our samples define a LMWL with a slope of 0.5271 (Figure 6(b)):

$$\ln(\delta^{17}O + 1) = 0.5271\ (\pm 0.0006)\ \ln(\delta^{18}O + 1) + 0.0154\ (\pm 0.0043)\ (R^{2} = 0.9999)$$

We also plot the data of the modern precipitation reported in the previous studies up to date, including those from this study (Figure 6(c)), and obtain a GMWL for $\ln(\delta^{17}O + 1)$ and $\ln(\delta^{18}O + 1)$:

$$\ln(\delta^{17}O + 1) = 0.5279\ (\pm 0.0001)\ \ln(\delta^{18}O + 1) + 0.0211\ (\pm 0.0011)\ (R^{2} = 1)$$

The slope of this GMWL agrees with that (0.528) of the GMWL proposed by Luz and Barkan (2010), although their result was based on a much smaller data set. The GMWL slope is about the same as the value (0.5275–0.5279) calculated under equilibrium fractionation conditions over the temperature range of 0–30°C (Barkan & Luz, 2007). The slope (0.5271) of our LMWL is only slightly shallower than the GMWL, suggesting that LMWLs in the tropics likely reflect conditions close to equilibrium. Like the LMWLs for $\delta^{18}O$ and $\delta^{2}H$, the slope of LMWLs for $\ln(\delta^{17}O + 1)$ and $\ln(\delta^{18}O + 1)$ also varies with geographic locations and gets higher with an

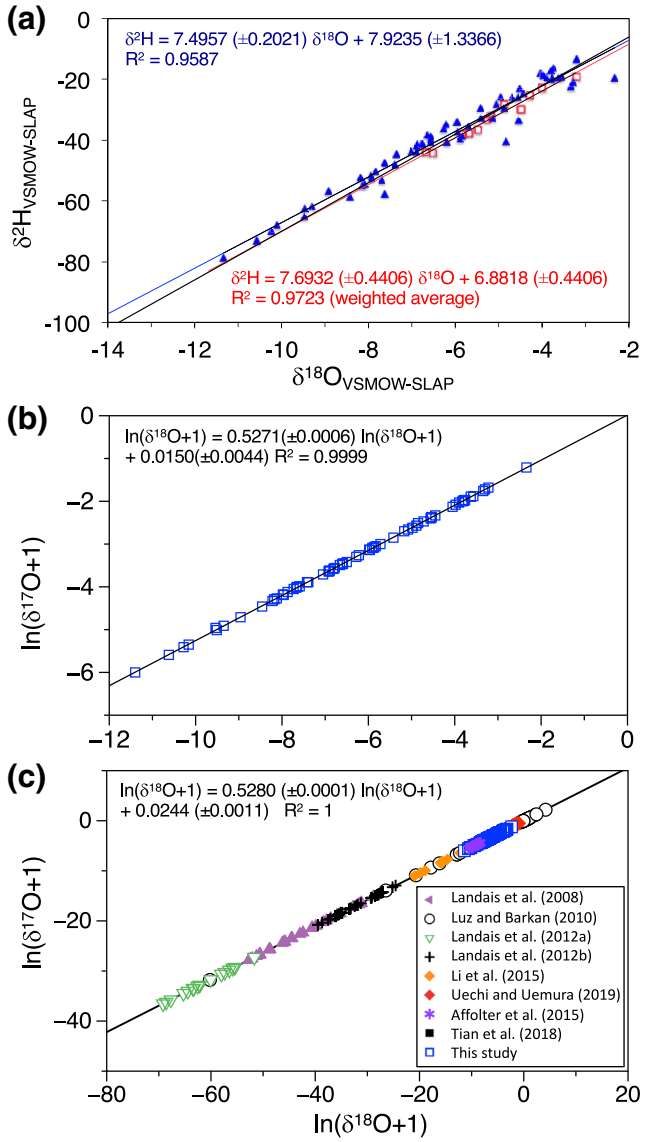

Figure 6. (a) Local meteoric water line from $\delta^{18}O$ and $\delta^{2}H$, (b) local meteoric water from $\ln(\delta^{18}O + 1)$ and $\ln(\delta^{17}O + 1)$, and (c) global meteoric water line from $\ln(\delta^{18}O + 1)$ and $\ln(\delta^{17}O + 1)$.

increase in latitude. For example, the slope increases to 0.5296 in a subtropical region (Uechi & Uemura, 2019) and further to 0.5299 in the polar regions (Landais, Ekaykin, et al., 2012). An even higher slope of 0.5310 can be obtained from an Antarctic ice core (Miller, 2018). Different slopes imply different hydrological conditions in different regions.

As pointed out by Uechi and Uemura (2019), the value of slope chosen can significantly affect the ^{17}O-excess calculation, especially in the polar region. If 0.5271 is used, ^{17}O-excess values of tropical and subtropical precipitation will be 1–10 per meg higher than the values obtained using 0.528 but still within the analytical error. However, for the polar region, ^{17}O-excess values will be 26–47 per meg higher. If 0.5299 is used, ^{17}O-excess values of tropical and subtropical regions will be 4–22 per meg lower, while ^{17}O-excess values for the polar region will be 55–100 per meg lower. The high sensitivity of ^{17}O-excess to the slope of meteoric water line in the polar region presents a real challenge to the interpretation of ^{17}O-excess, as the factors impacting ^{17}O-excess in high-latitude regions might be overstated (Miller, 2018; Uechi & Uemura, 2019). For the consistence of intercomparison, ^{17}O-excess still needs to be calculated with a slope of 0.528.

4.2. Controls of Monthly Precipitation $\delta^{18}O$

A weak correlation ($r = -0.31$, $p = 0.014$) between rainfall amount and $\delta^{18}O$ implies that amount effect is not a dominant driver of monthly precipitation $\delta^{18}O$ in our region. Datta et al. (1991) also noticed the lack of correlation between monthly isotope composition and rainfall in New Delhi. Aggarwal et al. (2004) found that precipitation isotopes are not correlated with the precipitation amount in regions impacted by the Asian monsoon. The amount effect, therefore, is not universal across tropical and subtropical regions.

Six-month seasonal variability in $\delta^{18}O$ results from the two monsoons (the SW monsoon and the NE monsoon) and the movement of the Intertropical Convergence Zone (ITCZ). The ITCZ passes the study area twice each year, and its timing matches the occurrences of the monsoons. The area is in the SW monsoon with the dominant southwesterly winds when the ITCZ moves from the south to the north, and in the NE monsoon with the dominant northeasterly winds when the ITCZ moves from the north to the south (Figure 2). $\delta^{18}O$ gradually becomes more negative during the monsoons and moves back to higher values when monsoons retreat. Although the spectral analysis does not reveal the clear periodicity of El Niño–Southern Oscillation (ENSO), its impact on precipitation isotopes is obvious. On the time series, $\delta^{18}O$ follows the variation of the ONI (Figure 3). When the ONI gets higher during an El Niño event, the average $\delta^{18}O$ also shifts to a relatively higher value. For example, during the El Niño event between 2015 and 2016, the average $\delta^{18}O$ value is −5.2‰ but during the following non-El Niño between 2016 and 2017, the average $\delta^{18}O$ value is much lower (−7.6‰, Table S1). Thus, ENSO impacts precipitation $\delta^{18}O$ on interannual time scale.

Monsoon and ENSO events drive $\delta^{18}O$ by affecting the regionally organized convective activities in frequency and intensity (He, Goodkin, Jackisch, et al., 2018; He, Goodkin, Kurita, et al., 2018). Regionally organized convection can significantly lower $\delta^{18}O$ values, while local convective activities have a limited impact on precipitation isotopes. The frequency and intensity of regionally organized convective activities increase with the monsoons, causing the negative excursions of $\delta^{18}O$. ENSO affects the monsoon driven convection in the region. During an El Niño event, warm water in the Western Pacific region moves eastward to the

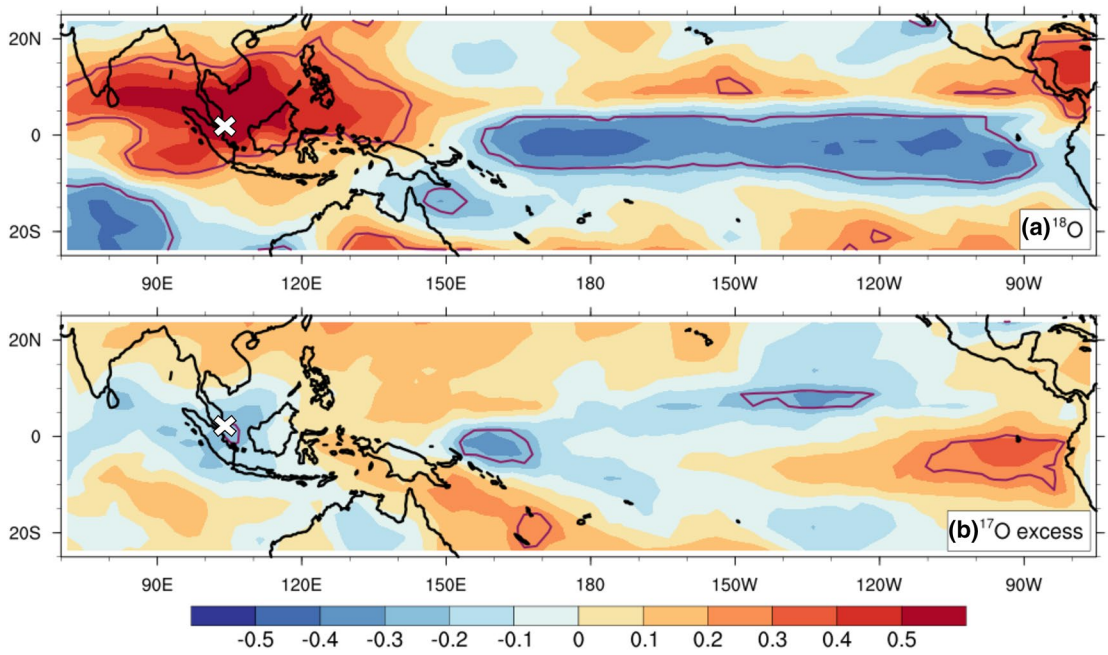

Figure 7. Correlation map of monthly $\delta^{18}O$ (a) and ^{17}O-excess (b) with outgoing longwave radiation (OLR). $\delta^{18}O$ shows a positive (inverse) correlation to OLR in SE Asia region (eastern Pacific), while ^{17}O-excess shows an inverse (positive) correlation to OLR in SE Asian (eastern Pacific). "×" represents the sampling site, and maroon contours indicate 95%confidence level of the correlation. SE, southeast.

eastern/central tropical pacific region, suppressing Walker Circulation associated convection in the Western Pacific and SE Asia. The La Niña event increases the strength of Walker Circulation and associated convection in the SE Asia. Precipitation $\delta^{18}O$, therefore, exhibits a strong correlation with regional convection as shown in the correlation map of $\delta^{18}O$ with OLR (Figure 7(a)).

4.3. ^{17}O-Excess, a Tracer of Moisture Source RH?

Both back trajectory analysis and reanalysis of moisture flux reveal the multiple moisture source regions for precipitation in our study area, including the SCS, the Indian Ocean, the Java Sea, and the Malacca Strait (Figures 2, 8, and S5; He, Goodkin, Jackisch, et al., 2018). Their relative contributions vary significantly between seasons, with the SCS being dominant during the NE monsoon. Therefore, it is easier to examine the correlation between ^{17}O-excess and RH of the source region (e.g., SCS) during the NE monsoon. If ^{17}O-excess largely reflects the RH of the SCS during the NE monsoon, change in precipitation ^{17}O-excess should follow the RH's variation. In addition, RH over the SCS would be significantly different during the 2013–2014 NE monsoon than the NE monsoons in the other years. Therefore, a higher average ^{17}O-excess value (Table S2) during 2013–2014 relative to other times would suggest low RH over the SCS. However, there was only a minor difference in RH over the SCS (Figure 9). By the same token, the extreme ^{17}O-excess value of 80 per meg observed in November 2018 would suggest an anomalously low RH or drought conditions in the source regions, contradicting the observations.

Furthermore, our statistical analysis shows no correlation between normalized RH of moisture source regions and ^{17}O-excess during the study period (Figure S6) and individual four seasons (Figure S7) even without the sample from November 2018. For example, during NE monsoon seasons, the correlation coefficient r between normalized RH of moisture sources and ^{17}O-excess is only 0.07 with $p = 0.74$.

The cause of the high ^{17}O-excess value in the sample from November 2018 is an enigma, and further investigation is needed. One possible explanation is the contribution of stratospheric water with high ^{17}O-excess (Lin et al., 2013; Pang et al., 2015). According to the Brewer–Dobson circulation, stratospheric air generally descends into the troposphere at midlatitudes and high latitudes (Lin et al., 2013). In the tropics, however,

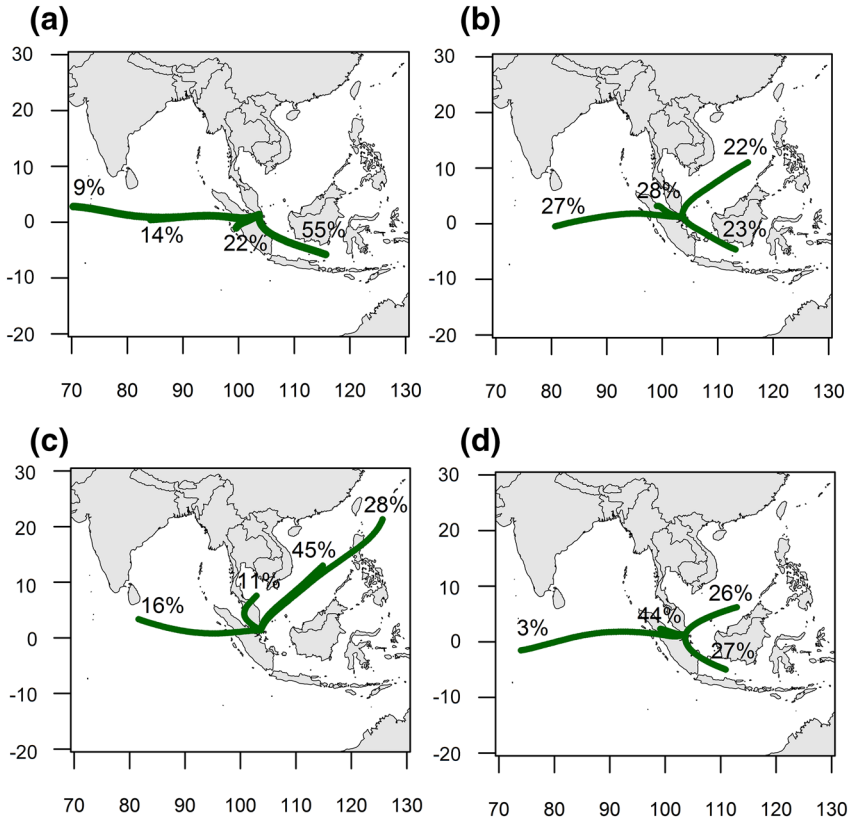

Figure 8. Cluster means of HYSPLIT's back trajectories during different seasons between 2013 and 2019: (a) June–September (SW monsoon), (b) October–November (intermonsoon), (c) December–March (NE monsoon), and (d) April–May (intermonsoon). HYSPLIT, Hybrid Single-particle Lagrangian Integrated Trajectory; SW, southwest; NE, northeast.

deep convection can reach beyond 15 km, where water vapor exchange between the troposphere and the stratosphere could happen. Note that this extreme value only appeared once in our record. While we can replicate the value from multiple measurements (Table S2), we tend to exclude it in further discussions before we could completely rule out sample abnormality.

Theoretical calculation and observations (Benetti et al., 2014) show that d-excess of water vapor is also negatively correlated to RH in source regions similar to the relationship between RH and ^{17}O-excess established experimentally (Barkan & Luz, 2007). If both d-excess and ^{17}O-excess in our samples largely record the RH of moisture source regions, we would expect that they are positively correlated. We however observed an anticorrelation between d-excess and ^{17}O-excess. Such a relationship implies that after source evaporation, transport, convection, and precipitation processes have modified these parameters and subsequently their correlations with the source region RH. d-Excess and especially ^{17}O-excess show no correlation with normalized RH in the source regions (Figure 10).

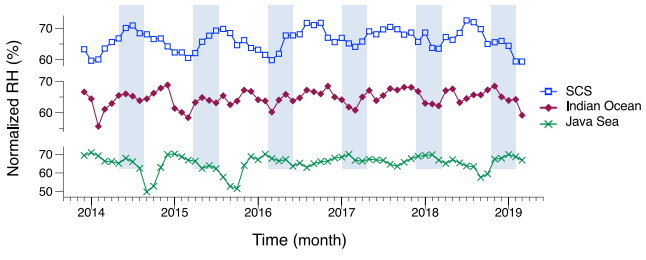

Figure 9. Normalized RH at the surface (1,000 hPa) of the major moisture sources in the South China Sea (SCS), the Indian Ocean, and the Java Sea during the study period. Normalized RH was calculated according to the procedure described in Schoenemann et al. (2014) and Uechi and Uemura (2019). Shaded periods are NE monsoons. RH, relative humidity; NE, northeast.

Landais et al. (2010) observed that both ^{17}O-excess and d-excess in African monsoon precipitation highly correlate to the low-level RH and thus proposed that RH is the key in controlling precipitation. Their simple reevaporation model well explains the correlation of ^{17}O-excess and d-excess with RH. In our study, however, only d-excess shows a weak correlation with on-site RH and RH at different atmospheric levels, and ^{17}O-excess does not correlate to the RH at all (Figures S2 and S3). This likely implies that rain reevaporation might not be a dominant process that affects isotopes, in particular, ^{17}O-excess in

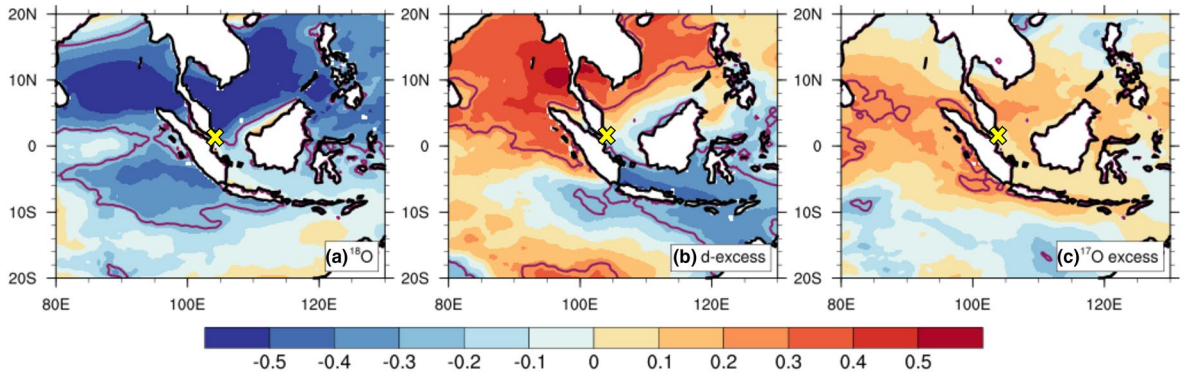

Figure 10. Correlation map of monthly $\delta^{18}O$ (a), d-excess (b), and ^{17}O-excess (c) with normalized RH in the moisture source regions in the SE Asia region. d-excess and ^{17}O-excess show very low or low correlation with RH in source regions. "×" represents the sampling site, and maroon contours indicate 95% confidence level of the correlation. RH, relative humidity; SE, southeast.

monthly precipitation. Risi et al. (2013) also investigated controls of the spatial–temporal distribution of d-excess and ^{17}O-excess in precipitation using the LMDZ GCM. Although ^{17}O-excess and d-excess are sensitive to the reevaporation parameter, they noticed that LMDX GCM cannot explain large seasonal variability of ^{17}O-excess observed in tropical regions, and thus processes rather than reevaporation, which are not captured by LMDZ, may be at play. Dütsch et al. (US CLIVAR Water Isotopes and Climate Workshop in 2019) quantified climatic controls on d-excess and ^{17}O-excess in Antarctica using iCAM5, an isotope-enabled atmosphere model. They decomposed the processes affecting d-excess and ^{17}O-excess into source region evaporation, transportation, and cloud formation. Their simulation shows that transport and cloud formation have opposite effects on d-excess and ^{17}O-excess, although they did not perform any further decomposition to investigate which specific processes exactly cause the opposite effects on these parameters. In addition, their study is limited in high latitudes. Previous GCM-based understanding of precipitation ^{17}O-excess in the tropics cannot explain our observations, and hence, further modeling investigation is necessary to elucidate the anticorrelation between d-excess and ^{17}O-excess.

Anticorrelation between ^{17}O-excess and d-excess is also found to change with the variation in regional convection. During non-El Niño years, ^{17}O-excess and d-excess are highly correlated with $r = -0.80$ and $p < 0.001$. Their anticorrection breaks down during El Niño years, when these two parameters are not correlated. Such behavior likely implies that the processes related to tropical convection affect ^{17}O-excess and d-excess, and their influence on ^{17}O-excess and d-excess varies with the intensity of regional convection in the area. During El Niño years, slowing atmospheric convection in SE Asia and the Western Pacific leads to a weakened monsoon in our study area. Correspondingly, the processes that affect ^{17}O-excess and d-excess likely have less impact on these two parameters.

^{17}O-excess shows strong periodicities at 3-month, 6-month, and 2.7-year 6-month periodicity indicates the impact of two alternating monsoons (the SW and NE monsoons). 2.7-Year periodicity can be related to ENSO variability. During our study period, two El Niño events (2015–2016 and 2018–2019) and two weak La Niña events (2016–2017 and 2017–2018) (https://origin.cpc.ncep.noaa.gov/products/analysis_monitoring/ensostuff/ONI_v5.php) were observed. However, as ENSO has 2–8 years of periodicity, a longer record is needed to fully understand the impact of ENSO variability on precipitation ^{17}O-excess. The 3-month periodicity likely represents intraseasonal oscillation in response to the Madden–Julian Oscillation (MJO). MJO is the dominant mode of intraseasonal variability in the tropics with a time scale of 30–90 days (Wheeler & Hendon, 2004; Zhang, 2005). In contrast, relatively weak periodic variations were observed in $\delta^{18}O$ and especially d-excess. This suggests that ^{17}O-excess can be used as a proxy for tropical climate variabilities, such as ENSO and monsoons, and thus, it can have significant implications for paleoclimate studies.

5. Conclusions

Tropical convection related to monsoons and ENSO is the dominant control of precipitation $\delta^{18}O$. A weak correlation ($r = -0.31$ and $p = 0.014$) between $\delta^{18}O$ and rainfall suggests that the amount effect has minimal influence on monthly precipitation $\delta^{18}O$ in our study area. $\delta^{18}O$ exhibits strong seasonal variability in response to the two monsoons and ITCZ movements in the SE Asia region; lower values are observed during the monsoons and high values appear during intermonsoon periods. Although the $\delta^{18}O$ time series is not long enough to reveal a robust periodicity with ENSO, its impact on $\delta^{18}O$ is noticeable. $\delta^{18}O$ follows the ONI; the average value is much higher during El Niño years than during non-El Niño years.

Longer records are needed to understand the correlation between ^{17}O-excess and ENSO, but our study reveals that ^{17}O-excess might be a good proxy for tropical climate variabilities such as ENSO and monsoons. Our samples generally have a consistent d-excess value of about 10 without clear periodicities. Compared to high-latitude regions, the samples in this study have a narrow range of ^{17}O-excess values, which mostly fall between 10 and 30 per meg, with an average of 21 ± 11 per meg, similar to that of precipitation in subtropical regions. Unlike d-excess and $\delta^{18}O$, the spectral analysis of ^{17}O-excess time series reveals significant 3-month, 6-month, and 2.7-year periodicities likely in response to intraseasonal oscillations (i.e., MJO), monsoons, and ENSO, respectively.

These LMWLs defined by ^{18}O and $\delta^{2}H$ have slopes and intercepts shallower than that of GMWL, suggesting the influence of subcloud evaporation of raindrops in tropical precipitation. The LMWL defined by $\ln(\delta^{17}O + 1)$ and $\ln(\delta^{18}O + 1)$ of our samples has a slope (0.5271) slightly shallower than that (0.5278) of the GMWL and much shallower than the LMWLs from midlatitude and high-latitude regions.

Further modeling studies are needed to explore which process(es) during convection can alter ^{17}O-excess and d-excess and lead to the anticorrelation between these two parameters. Variations in both d-excess and ^{17}O-excess do not follow the RH in ocean moisture source regions. Extremely dry conditions in moisture source regions are required to explain those samples with high ^{17}O-excess values. Furthermore, an anticorrelation exists between ^{17}O-excess and d-excess breaks down during El Niño periods. Therefore, tropical convection significantly affects ^{17}O-excess and d-excess, particularly ^{17}O-excess, which no longer record RH of moisture source regions.

Acknowledgments
The authors would like to thank P. Polivka and other colleagues in the Climate group at EOS for collecting samples while we were away. Dr R.D. Ramos did the spectral analysis for this research, Mr Q.B. Shi and Dr Zhaoquan Huang helped to make the regional map. Constructive and critical comments from three anonymous reviewers greatly improved the manuscript. We thank Dr Chidong Zhang, the Editor, for his effort in facilitating its review during this Pandemic. This research is supported by the National Research Foundation Singapore and the Singapore Ministry of Education under the Research Centres of Excellence initiative. It comprises Earth Observatory of Singapore contribution no. 273. The partial financial support is provided by the NRF-NSFC joint grant (NRF2017NRF-NSFC001-047 to X.W.). This research is also the part of IAEA Coordinated Research Project (CRP Code: F31004) on "Stable isotopes in precipitation and paleoclimatic archives in tropical areas to improve regional hydrological and climatic impact model" with IAEA Research Agreement No. 17980.

Data Availability Statement

Monthly precipitation samples and their isotope values (including d-excess and ^{17}O-excess), with the corresponding on-site meteorological parameters, are listed in Table S2. The data are also available at https://figshare.com/s/6e9c464b1c6a25fb7b63. Other observational and reanalysis data sets are freely available from their respective sites as mentioned in the text.

References

Aemisegger, F., Pfahl, S., Sodemann, H., Lehner, I., Seneviratne, S. I., & Wernli, H. (2014). Deuterium excess as a proxy for continental moisture recycling and plant transpiration. *Atmospheric Chemistry and Physics*, *14*(8), 4029–4054. https://doi.org/10.5194/acp-14-4029-2014

Aggarwal, P. K., Fröhlich, K., Kulkarni, K. M., & Gourcy, L. L. (2004). Stable isotope evidence for moisture sources in the Asian summer monsoon under present and past climate regimes. *Geophysical Research Letters*, *31*, L08203. https://doi.org/10.1029/2004GL019911

Angert, A., Cappa, C. D., & DePaolo, D. J. (2004). Kinetic ^{17}O effects in the hydrologic cycle: Indirect evidence and implications. *Geochimica et Cosmochimica Acta*, *68*(17), 3487–3495. https://doi.org/10.1016/j.gca.2004.02.010

Barkan, E., & Luz, B. (2005). High precision measurements of $^{17}O/^{16}O$ and $^{18}O/^{16}O$ ratios in H_2O. *Rapid Communications in Mass Spectrometry*, *19*(24), 3737–3742. https://doi.org/10.1002/rcm.2250

Barkan, E., & Luz, B. (2007). Diffusivity fractionations of $H_2{}^{16}O/H_2{}^{17}O$ and $H_2{}^{16}O/H_2{}^{18}O$ in air and their implications for isotope hydrology. *Rapid Communications in Mass Spectrometry*, *21*(18), 2999–3005. https://doi.org/10.1002/rcm.3180

Benetti, M., Reverdin, G., Pierre, C., Merlivat, L., Risi, C., Steen-Larsen, H. C., & Vimeux, F. (2014). Deuterium excess in marine water vapor: Dependency on relative humidity and surface wind speed during evaporation. *Journal of Geophysical Research: Atmospheres*, *119*, 584–593. https://doi.org/10.1002/2013JD020535

Cheng, H., Edwards, R. L., Sinha, A., Spötl, C., Yi, L., Chen, S., et al. (2016). The Asian monsoon over the past 640,000 years and ice age terminations. *Nature*, *534*(7609), 640–646. https://doi.org/10.1038/nature18591

Craig, H. (1961). Isotopic variations in meteoric waters. *Science*, *133*(3465), 1702. https://doi.org/10.1126/science.133.3465.1702

Dansgaard, W. (1964). Stable isotopes in precipitation. *Tellus*, *16*(4), 436–468. https://doi.org/10.1111/j.2153-3490.1964.tb00181.x

Datta, P. S., Tyagi, S. K., & Chandrasekharan, H. (1991). Factors controlling stable isotope composition of rainfall in New Delhi, India. *Journal of Hydrology*, *128*(1), 223–236. https://doi.org/10.1016/0022-1694(91)90139-9

Gröning, M., Lutz, H. O., Roller-Lutz, Z., Kralik, M., Gourcy, L., & Pöltenstein, L. (2012). A simple rain collector preventing water re-evaporation dedicated for $\delta^{18}O$ and $\delta^{2}H$ analysis of cumulative precipitation samples. *Journal of Hydrology*, *448–449*(Suppl. C), 195–200. https://doi.org/10.1016/j.jhydrol.2012.04.041

He, S., Goodkin, N. F., Jackisch, D., Ong, M. R., & Samanta, D. (2018). Continuous real-time analysis of the isotopic composition of precipitation during tropical rain events: Insights into tropical convection. *Hydrological Processes*, *32*(11), 1531–1545. https://doi.org/10.1002/hyp.11520

He, S., Goodkin, N. F., Kurita, N., Wang, X., & Rubin, C. M. (2018). Stable isotopes of precipitation during tropical Sumatra squalls in Singapore. *Journal of Geophysical Research: Atmospheres*, *123*, 3812–3829. https://doi.org/10.1002/2017JD027829

Hoffmann, G., Ramirez, E., Taupin, J. D., Francou, B., Ribstein, P., Delmas, R., et al. (2003). Coherent isotope history of Andean ice cores over the last century. *Geophysical Research Letters*, *30*(4), 1179. https://doi.org/10.1029/2002GL014870

Jouzel, J. (2003). Water stable isotopes: Atmospheric composition and applications in polar ice core studies. In H. D. Holland & K. K. Turekian (Ed.), *Treatise on geochemistry* (pp. 213–243). Oxford, UK: Pergamon. https://doi.org/10.1016/B0-08-043751-6/04040-8

Jouzel, J., Delaygue, G., Landais, A., Masson-Delmotte, V., Risi, C., & Vimeux, F. (2013). Water isotopes as tools to document oceanic sources of precipitation: Water isotopes and precipitation origin. *Water Resources Research*, *49*, 7469–7486. https://doi.org/10.1002/2013WR013508

Jouzel, J., Merlivat, L., & Lorius, C. (1982). Deuterium excess in an East Antarctic ice core suggests higher relative humidity at the oceanic surface during the last glacial maximum. *Nature*, *299*(5885), 688–691. https://doi.org/10.1038/299688a0

Klein, E. S., Nolan, M., McConnell, J., Sigl, M., Cherry, J., Young, J., & Welker, J. M. (2016). McCall Glacier record of Arctic climate change: Interpreting a northern Alaska ice core with regional water isotopes. *Quaternary Science Reviews*, *131*, 274–284. https://doi.org/10.1016/j.quascirev.2015.07.030

Kurita, N., Ichiyanagi, K., Matsumoto, J., Yamanaka, M. D., & Ohata, T. (2009). The relationship between the isotopic content of precipitation and the precipitation amount in tropical regions. *Isoscapes: Isotope Mapping and Its Applications*, *102*(3), 113–122. https://doi.org/10.1016/j.gexplo.2009.03.002

Landais, A., Barkan, E., & Luz, B. (2008). Record of $\delta^{18}O$ and ^{17}O-excess in ice from Vostok Antarctica during the last 150,000 years. *Geophysical Research Letters*, *35*, L02709. https://doi.org/10.1029/2007GL032096

Landais, A., Ekaykin, A., Barkan, E., Winkler, R., & Luz, B. (2012). Seasonal variations of ^{17}O-excess and d-excess in snow precipitation at Vostok station, East Antarctica. *Journal of Glaciology*, *58*(210), 725–733. https://doi.org/10.3189/2012JoG11J237

Landais, A., Risi, C., Bony, S., Vimeux, F., Descroix, L., Falourd, S., & Bouygues, A. (2010). Combined measurements of ^{17}O-excess and d-excess in African monsoon precipitation: Implications for evaluating convective parameterizations. *Earth and Planetary Science Letters*, *298*(1), 104–112. https://doi.org/10.1016/j.epsl.2010.07.033

Landais, A., Steen-Larsen, H. C., Guillevic, M., Masson-Delmotte, V., Vinther, B., & Winkler, R. (2012). Triple isotopic composition of oxygen in surface snow and water vapor at NEEM (Greenland). *Geochimica et Cosmochimica Acta*, *77*(Suppl. C), 304–316. https://doi.org/10.1016/j.gca.2011.11.022

Lee, J.-E., Fung, I., DePaolo, D. J., & Henning, C. C. (2007). Analysis of the global distribution of water isotopes using the NCAR atmospheric general circulation model. *Journal of Geophysical Research*, *112*, D16306. https://doi.org/10.1029/2006JD007657

Lekshmy, P. R., Midhun, M., Ramesh, R., & Jani, R. A. (2014). ^{18}O depletion in monsoon rain relates to large scale organized convection rather than the amount of rainfall. *Scientific Reports*, *4*, 5661. https://doi.org/10.1038/srep05661

Li, S., Levin, N. E., & Chesson, L. A. (2015). Continental scale variation in ^{17}O-excess of meteoric waters in the United States. *Geochimica et Cosmochimica Acta*, *164*(Suppl. C), 110–126. https://doi.org/10.1016/j.gca.2015.04.047

Lin, Y., Clayton, R. N., Huang, L., Nakamura, N., & Lyons, J. R. (2013). Oxygen isotope anomaly observed in water vapor from Alert, Canada and the implication for the stratosphere. *Proceedings of the National Academy of Sciences*, *110*(39), 15608–15613. https://doi.org/10.1073/pnas.1313014110

Lo, J. C.-F., & Orton, T. (2016). The general features of tropical Sumatra Squalls. *Weather*, *71*(7), 175–178. https://doi.org/10.1002/wea.2748

Luz, B., & Barkan, E. (2010). Variations of $^{17}O/^{16}O$ and $^{18}O/^{16}O$ in meteoric waters. *Geochimica et Cosmochimica Acta*, *74*(22), 6276–6286. https://doi.org/10.1016/j.gca.2010.08.016

Merlivat, L., & Jouzel, J. (1979). Global climatic interpretation of the deuterium–oxygen 18 relationship for precipitation. *Journal of Geophysical Research*, *84*(C8), 5029–5033. https://doi.org/10.1029/JC084iC08p05029

Miller, M. F. (2018). Precipitation regime influence on oxygen triple-isotope distributions in Antarctic precipitation and ice cores. *Earth and Planetary Science Letters*, *481*, 316–327. https://doi.org/10.1016/j.epsl.2017.10.035

Moerman, J. W., Cobb, K. M., Adkins, J. F., Sodemann, H., Clark, B., & Tuen, A. A. (2013). Diurnal to interannual rainfall $\delta^{18}O$ variations in northern Borneo driven by regional hydrology. *Earth and Planetary Science Letters*, *369–370*(Suppl. C), 108–119. https://doi.org/10.1016/j.epsl.2013.03.014

Munksgaard, N. C., Kurita, N., Sánchez-Murillo, R., Ahmed, N., Araguas, L., Balachew, D. L., et al. (2019). Data descriptor: Daily observations of stable isotope ratios of rainfall in the tropics. *Scientific Reports*, *9*, 14419. https://doi.org/10.1038/s41598-019-50973-9

Paillard, D., Labeyrie, L., & Yiou, P. (1996). Macintosh Program performs time-series analysis. *Eos, Transactions American Geophysical Union*, *77*(39), 379. https://doi.org/10.1029/96EO00259

Pang, H., Hou, S., Landais, A., Masson-Delmotte, V., Prie, F., Steen-Larsen, H. C., et al. (2015). Spatial distribution of ^{17}O-excess in surface snow along a traverse from Zhongshan station to Dome A, East Antarctica. *Earth and Planetary Science Letters*, *414*(Suppl. C), 126–133. https://doi.org/10.1016/j.epsl.2015.01.014

Risi, C., Bony, S., & Vimeux, F. (2008). Influence of convective processes on the isotopic composition ($\delta^{18}O$ and δD) of precipitation and water vapor in the tropics: 2. Physical interpretation of the amount effect. *Journal of Geophysical Research*, *113*, D19306. https://doi.org/10.1029/2008JD009943

Risi, C., Bony, S., Vimeux, F., & Jouzel, J. (2010). Water-stable isotopes in the LMDZ4 general circulation model: Model evaluation for present-day and past climates and applications to climatic interpretations of tropical isotopic records. *Journal of Geophysical Research*, *115*, D12118. https://doi.org/10.1029/2009JD013255

Risi, C., Landais, A., Winkler, R., & Vimeux, F. (2013). Can we determine what controls the spatio-temporal distribution of d-excess and ^{17}O-excess in precipitation using the LMDZ general circulation model? *Climate of the Past*, *9*(5), 2173–2193. https://doi.org/10.5194/cp-9-2173-2013

Rozanski, K., Araguás-Araguás, L., & Gonfiantini, R. (1993). Isotopic patterns in modern global precipitation. In *Climate change in continental isotopic records* (pp. 1–36). American Geophysical Union. https://doi.org/10.1029/GM078p0001

Schoenemann, S. W., Schauer, A. J., & Steig, E. J. (2013). Measurement of SLAP2 and GISP $\delta^{17}O$ and proposed VSMOW-SLAP normalization for $\delta^{17}O$ and $^{17}O_{excess}$: Measurement of SLAP2 and GISP $\delta^{17}O$ values. *Rapid Communications in Mass Spectrometry*, *27*(5), 582–590. https://doi.org/10.1002/rcm.6486

Schoenemann, S. W., & Steig, E. J. (2016). Seasonal and spatial variations of $^{17}O_{excess}$ and d_{excess} in Antarctic precipitation: Insights from an intermediate complexity isotope model. *Journal of Geophysical Research: Atmospheres*, *121*, 11215–11247. https://doi.org/10.1002/2016JD025117

Schoenemann, S. W., Steig, E. J., Ding, Q., Markle, B. R., & Schauer, A. J. (2014). Triple water-isotopologue record from WAIS Divide, Antarctica: Controls on glacial–interglacial changes in $^{17}O_{excess}$ of precipitation: WAIS LGM-Holocene $^{17}O_{excess}$ Record. *Journal of Geophysical Research: Atmospheres*, *119*, 8741–8763. https://doi.org/10.1002/2014JD021770

Steig, E. J., Gkinis, V., Schauer, A. J., Schoenemann, S. W., Samek, K., Hoffnagle, J., et al. (2014). Calibrated high-precision ^{17}O-excess measurements using cavity ring-down spectroscopy with laser-current-tuned cavity resonance. *Atmospheric Measurement Techniques*, *7*(8), 2421–2435. https://doi.org/10.5194/amt-7-2421-2014

Stein, A. F., Draxler, R. R., Rolph, G. D., Stunder, B. J. B., Cohen, M. D., & Ngan, F. (2015). NOAA's HYSPLIT atmospheric transport and dispersion modeling system. *Bulletin of the American Meteorological Society*, *96*(12), 2059–2077. https://doi.org/10.1175/BAMS-D-14-00110.1

Stenni, B. (2001). An oceanic cold reversal during the last deglaciation. *Science*, *293*(5537), 2074–2077. https://doi.org/10.1126/science.1059702

Tian, C., Wang, L., Kaseke, K. F., & Bird, B. W. (2018). Stable isotope compositions (δ^2H, $\delta^{18}O$ and $\delta^{17}O$) of rainfall and snowfall in the central United States. *Scientific Reports*, *8*, 6712. https://doi.org/10.1038/s41598-018-25102-7

Tremoy, G., Vimeux, F., Soumana, S., Souley, I., Risi, C., Favreau, G., & Oï, M. (2014). Clustering mesoscale convective systems with laser-based water vapor $\delta^{18}O$ monitoring in Niamey (Niger). *Journal of Geophysical Research: Atmospheres*, *119*, 5079–5103. https://doi.org/10.1002/2013JD020968

Uechi, Y., & Uemura, R. (2019). Dominant influence of the humidity in the moisture source region on the 17O-excess in precipitation on a subtropical island. *Earth and Planetary Science Letters*, *513*, 20–28. https://doi.org/10.1016/j.epsl.2019.02.012

van Geldern, R., & Barth, J. A. C. (2012). Optimization of instrument setup and post-run corrections for oxygen and hydrogen stable isotope measurements of water by isotope ratio infrared spectroscopy (IRIS). *Limnology and Oceanography: Methods*, *10*(12), 1024–1036. https://doi.org/10.4319/lom.2012.10.1024

Vimeux, F., Masson, V., Delaygue, G., Jouzel, J., Petit, J. R., & Stievenard, M. (2001). A 420,000 year deuterium excess record from East Antarctica: Information on past changes in the origin of precipitation at Vostok. *Journal of Geophysical Research*, *106*, 31863–31873. https://doi.org/10.1029/2001JD900076

Vimeux, F., Tremoy, G., Risi, C., & Gallaire, R. (2011). A strong control of the South American SeeSaw on the intra-seasonal variability of the isotopic composition of precipitation in the Bolivian Andes. *Earth and Planetary Science Letters*, *307*(1), 47–58. https://doi.org/10.1016/j.epsl.2011.04.031

Voss, K. A., Bookhagen, B., Sachse, D., & Chadwick, O. A. (2018). Variation of deuterium excess in surface waters across a 5000-m elevation gradient in the east-central Himalaya. *Hydrology and Earth System Sciences Discussions*, 1–20. https://doi.org/10.5194/hess-2018-534

Wheeler, M. C., & Hendon, H. H. (2004). An all-season real-time multivariate MJO index: Development of an index for monitoring and prediction. *Monthly Weather Review*, *132*, 16.

Winkler, R., Landais, A., Sodemann, H., Dümbgen, L., Prié, F., Masson-Delmotte, V., et al. (2012). Deglaciation records of ^{17}O-excess in East Antarctica: Reliable reconstruction of oceanic normalized relative humidity from coastal sites. *Climate of the Past*, *8*(1), 1–16. https://doi.org/10.5194/cp-8-1-2012

Zhang, C. (2005). Madden–Julian oscillation. *Reviews of Geophysics*, *43*, RG2003. https://doi.org/10.1029/2004RG000158